



# Soft x-ray Ar<sup>+8</sup> laser excited by low-voltage capillary discharge

B. FEKETE,<sup>1</sup> M. KISS,<sup>1</sup> A. A. SHAPOLOV,<sup>2</sup> S. SZATMARI,<sup>3</sup> AND S. V. KUKHLEVSKY<sup>1,\*</sup> 

<sup>1</sup>*Department of Computational Physics, Institute of Physics, University of Pecs, Ifjusag str. 6, 7624 Pecs, Hungary*

<sup>2</sup>*Laboratory of 3D Functional Network and Dendritic Imaging, Institute of Experimental Medicine, Tuzolto 7 str. 59, 1094 Budapest, Hungary*

<sup>3</sup>*Department of Experimental Physics, University of Szeged, Dom ter 9, 6720 Szeged, Hungary*

\*[feketebalazs@fizika.ttk.pte.hu](mailto:feketebalazs@fizika.ttk.pte.hu)

**Abstract:** We demonstrated the operation of a 46.9-nm capillary discharge Ar<sup>+8</sup>-laser excited by electrical pulses at a very low voltage (35 – 45 kV), which is approximately two times lower than previously reported. The decrease in pulse voltage not only allows for further reduction in the size of the laser's excitation part, but also a principal shift to the experimental methods, techniques, and technologies used in ordinary pulsed gas lasers operating in the ultraviolet, visible, and infrared regions of the spectra. In an argon-filled alumina capillary with an inner diameter of 3.1 mm and a length of 22 cm, laser pulses with an energy of 4 μJ and a duration of 1.6 ns were generated. The laser produces a beam with a Gaussian intensity distribution and an FWHM divergence of 1.9 mrad. The results could be particularly useful in the development of compact, practical soft x-ray capillary lasers for use in small laboratories at educational and research institutions.

© 2023 Optica Publishing Group under the terms of the [Optica Open Access Publishing Agreement](#)

## 1. Introduction

Plasma-based soft x-ray lasers [1–3] are important for a variety of applications in science and technology, such as diagnostics of hot-dense plasmas, photochemistry, nanoscale material ablation, optical constant measurement, characterizing soft x-ray optics, color center creation in crystals, nanoscale imaging, holography, and nanoscale defect-free patterning (see, for example, [4–11] and references therein). One of the most perspective soft x-ray lasers is the 46.9-nm Ar<sup>+8</sup>-laser with capillary discharge excitation [12–29].

Since the first demonstration of a 46.9-nm Ar<sup>+8</sup> laser excited by capillary Z-pinch discharge [12], several research groups have been able to create such a laser system [13–29]. The laser arrangement [12] was considered by all the research groups to be the reference system, and their own systems have followed the scheme outlined in this article. The system employs a water capacitor that is pulsed charged by a high-voltage (0.2 – 0.8 MV) Marx generator. The design and operation of such a system necessitate knowledge of Z-pinch thermonuclear fusion physics and particle acceleration high-voltage techniques rather than conventional discharge-pumped lasers. Marx generators are complex, time-consuming to maintain, and unsuitable for mass production. In 2005, the study [16] demonstrated a Marx-generator-free laser with an operating voltage in the range 80 – 90 kV that is benchtop-sized and capable of producing 46.9-nm pulses at a pulse repetition rate 12 Hz with an energy of 13 μJ, FWHM duration of 1.5 ns, and an annular-shape beam profile with peak-to-peak divergence of 5.2 mrad. The relatively low voltage required for its operation simplified the excitation system by utilizing ceramic capacitors and allowed a reduction of nearly one order of magnitude in the size of the pulsed power unit compared to previously reported capillary discharge Ar<sup>+8</sup> lasers. This type of Ar<sup>+8</sup> laser is less expensive and portable

enough to be installed in educational and research institutions' small laboratories for use in many scientific and application fields, complementing large-scale free electron laser facilities.

The present study demonstrates the operation of a 46.9-nm capillary discharge  $\text{Ar}^{+8}$  laser excited by ceramic capacitors charged to a very low voltage (35 – 45 kV), which is about twice as low as previously reported. The decrease in pulse voltage not only enables a further reduction in the size of the laser's excitation part but also a fundamental switch to the experimental approaches, techniques, and technologies widely employed in pulsed transversally excited atmospheric (TEA) gas lasers (XeCl,  $\text{CO}_2$ , et al.) operating in the long-wavelength regions of the spectra. By using such standard techniques, more laboratories will be able to conduct further research on soft x-ray capillary lasers, especially those that would operate at wavelengths shorter than 46.9 nm. The reduction of pulse voltage to 35 – 45 kV has approached the operating voltage of semiconductor technologies, which could theoretically lead to the miniaturization of the  $\text{Ar}^{+8}$ -laser system. In such a case, one can take advantage of magneto-electric confinement and stabilization of the plasma column in a pre-ionization-unit-free  $\text{Ar}^{+8}$  laser, which is excited by a capillary Z pinch via the combined magnetic and electric fields of the gliding surface discharge [24]. In the current study, the pumping unit, which is based on that generally used in discharge-pumped gas lasers (e.g., Lambda Physik excimer lasers of the LPX series), was used to generate laser pulses with 4  $\mu\text{J}$  of energy and an FWHM duration of 1.6 ns in an argon-filled alumina capillary with an inner diameter of 3.1 mm and a length of 22 cm. The laser generates a beam with a Gaussian intensity distribution and a 1.9 mrad FWHM divergence. The findings could be particularly useful in the research and development of compact, affordable soft x-ray capillary lasers for use in small laboratories at educational and research institutions.

The following is how the current paper is structured: The second section describes the experimental setup and diagnostics of a 46.9-nm capillary discharge  $\text{Ar}^{+8}$ -laser excited by very low-voltage pulses (35 – 45 kV). Section 3 contains the experimental results and their discussions. Section 4 presents a summary, conclusions, and plans for further experimental and theoretical investigations of the novel (35 – 45 kV) regime of laser excitation.

## 2. Experimental set-up and diagnostics

For the operation of an  $\text{Ar}^{+8}$  laser driven by capillary Z pinch discharges, numerous physical processes and discharge parameters are critical [1–29]. Lasing on the 46.9 nm line of the  $2p^53p(J=0) - 2p^53s(J=1)$  transition of neon-like argon is achieved in the hot ( $T_e \sim 100$  eV) and dense ( $N_e \sim 10^{18} \text{ cm}^{-3}$ ) plasma of a capillary Z pinch. The hot, dense, and highly ionized plasma column with a diameter of 150 – 300  $\mu\text{m}$  and length up to 0.5 m is produced by a longitudinal, high-current ( $I > 10$  kA) electric discharge with a short (100 – 200 ns) half-period in an  $\text{Al}_2\text{O}_3$ -ceramic capillary channel with a diameter of 3 – 4 mm initially filled with low-pressure (0.1 – 0.6 mbar) argon gas. The electron temperature ( $T_e$ ) and density ( $N_e$ ) are increased by fast radial compression (Z pinch) of the plasma column caused by the magnetic field of the current pulse and high thermal pressure gradients near the capillary wall. For pre-ionization of the Ar gas, a current pulse with an amplitude more than  $\sim 20$  A and a duration greater than  $\sim 3$   $\mu\text{s}$  is switched before the main high-current pulse. This does provide uniform confinement and compression of the plasma column by ensuring uniform starting conditions. Deviations in the discharge conditions result in the failure of lasing.

To provide the plasma parameters required for excitation of a 46.9-nm capillary discharge  $\text{Ar}^{+8}$  laser, we used the excitation circuit shown in Fig. 1(a). This is based on the extensively used electric excitation scheme of excimer lasers, where our group has long-time experience fulfilling the special pumping requirements of large-aperture, short-pulse excimer amplifiers, together with the construction of the corresponding preionization schemes [30,31]. In the current study, we used a standard, thyatron-driven (Lambda Physik LP-189) L-C inversion circuit, completed by magnetic switch compressor (MSC) technology. For the given value of the main capacitor

bank ( $C_1 = C_2 = 80$  nF, determined by the electric energy to be transferred), the inversion time is synchronized to the switching of the MSC by the proper choice of  $L$  and the cross section of the core of the MSC (Metglas 2605 Co) surrounded by a “spatially distributed coil” of one winding. The peaking capacitance  $C_3 = 44$  nF is distributed around the axis of the spark gap and the capillary-discharge chamber of cylindrical geometry. With the use of this charging circuit, a 50 kV electric pulse with a 120 ns rise time could be produced on the cathode electrode at a power supply voltage of  $U_0 = 27$  kV. The temporal behavior of this pulse (curve  $U$ ) is shown in Fig. 2 at  $U_0 = 27$  kV. Curve  $I$  is the discharge current, which is picked up in the  $C_3$  of the spark-gap-capillary circuit (see later). The main advantage of this excitation scheme (allowing as low as a 50 kV excitation electric pulse for reliable operation of the capillary laser) is given by the fast rise of the voltage on the peaking capacitor, as seen from the curve  $U$  of Fig. 2. It is known from our former experience with electric discharges that such a fast rising and pre-pulse-free voltage can create or drive a stable, low-impedance discharge, whose start of operation can properly be delayed to temporally match the maximum of the voltage on the capacitor (the  $C_3$  peaking capacitor in our case). In connection with this criteria, the pre-pulse of the pre-ionization unit (see later) generates a voltage on the electrodes of the spark gap prior to the main excitation pulse, which has an influence on its operation. This effect on the stable operation and exact timing of the spark gap is presently studied by us, using a pre-pulse compensation unit (also indicated in Fig. 1(a)). Corresponding results, and a detailed description of the circuits will be published elsewhere. The fast slope of the voltage on  $C_3$  is an indication of the fast rise of the current in the  $C_3$ , spark gap, and capillary circuit.

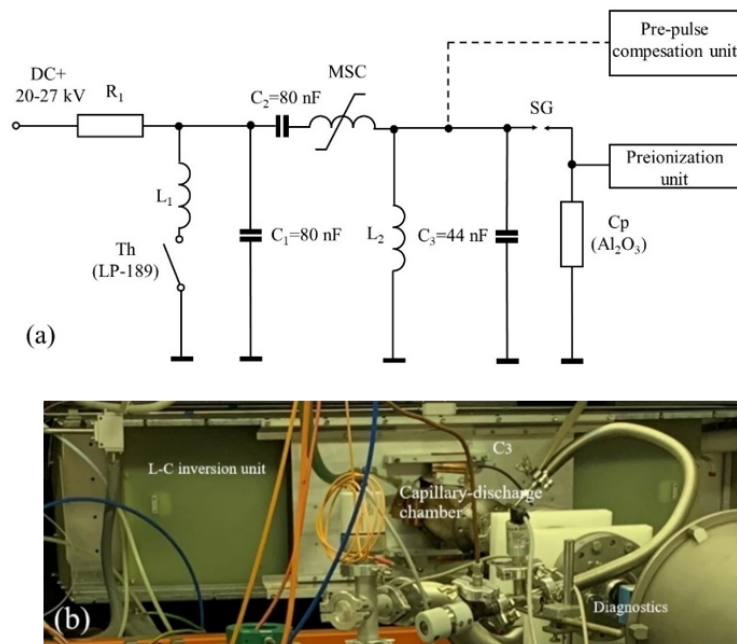


**Fig. 1.** (a) Schematics of the charging circuit based on the L-C inversion and magnetic switch compressor (MSC) of the 46-nm capillary discharge  $A^{r+8}$  laser with voltage inversion on capacitor  $C_1$ . The peaking capacitor  $C_3$  is charged to the voltage 35 – 45 kV. (b) Photograph of the pumping unit and laser head.

The capacitor  $C_3$  is discharged using a low-inductance coaxial discharge configuration via a pressurized air spark-gap switch connected in series with the capillary load. The design is similar to [16], except for the employment of a magnetic switch and the fact that the spark

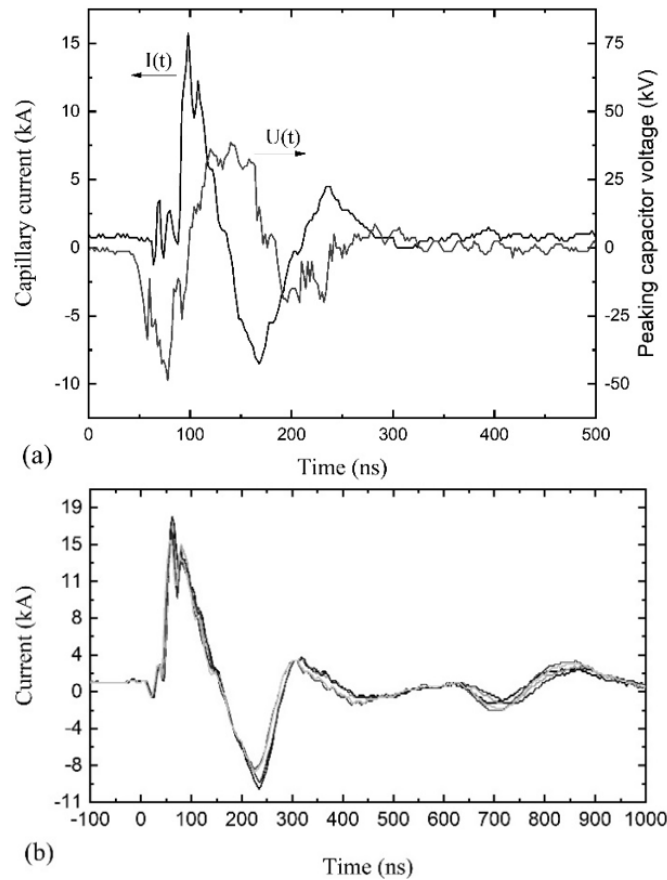


**Fig. 2.** (a) The current ( $I$ ) and voltage ( $U$ ) pulses measured by the shunt resistor; (b) Five current pulses showing the shot-to-shot stability.

gap is located on the axis of the discharge configuration. In comparison to the previous study [16], such an arrangement minimizes the rising time of the excitation current while increasing excitation efficiency. Furthermore, the low voltage does not necessitate the use of transformer oil for electrical isolation of the excitation system. Figure 1(b) depicts a photograph of the entire pumping system, which includes the laser head (capillary). One can compare that to the photograph [16] of the laser chamber, which shows the spark gap, peaking capacitor, and capillary. It should be emphasized that the current study addresses lasers operating in a novel (low-voltage) domain that allows for the reduction of the whole laser system rather than describing a concrete laser device. In the current (experimental) device, we did not use the smallest commercially available ceramic capacitors for further minimization of the dimensions of the whole laser system or even for its miniaturization by using semiconductor technologies and/or the advantage of magneto-electric confinement and stabilization of the plasma column in a pre-ionization-unit-free laser scheme [24]. The spark gap is adjusted so that the discharge takes place at the maximum voltage (Fig. 1(a)). The lasing is obtained in an  $\text{Al}_2\text{O}_3$  ceramic capillary with an internal diameter of 3.1 mm and a length of 22 cm that is filled with continuously flowing argon gas at 0.18 – 0.24 mbar. The excitation current pulse has a peak value up to 17 kA, a 10% to 90% rise time of approximately 15 ns, and a first half cycle duration of approximately 200 ns, as measured by a Rogowsky coil or low-inductance shunt resistor. Figure 2 depicts a typical current pulse measured

by a shunt resistor connected in parallel with the cathode electrode. The use of a shunt resistor was chosen due to the low voltage (35 – 45 kV) from the experimental methods employed in ordinary TEA-gas pulsed lasers.

The main discharge pulse is preceded by a 25  $\mu$ s-long current pulse with an amplitude of 20 A, which pre-ionizes the gas, ensuring uniform initial conditions (see also Fig. 1). The 46.9 nm laser line was recorded using a Jobin-Yvon spectrometer attached to a microchannel plate charge-coupled device detection system or directly to the phosphor screen. A fast vacuum X-ray photodiode (rise time of  $\sim$ 0.2 ns) with a gold photocathode was used to measure the temporal characteristics and energy of the laser pulse. The quantum efficiency of the photocathode was calibrated using a commercially available XRD (SXUV 100A1). To avoid space charge saturation between the cathode and the anode mesh, the cathode was polarized with respect to the grounded anode by a 0.5 kV negative voltage. The far-field intensity distributions of the laser pulses were recorded using a phosphor screen coupled to a CCD camera without and with a 0.4  $\mu$ m thick Al-foil intensity attenuator. A 100 MHz digital oscilloscope (TDS1012) was used for signal analysis. For more details on the diagnostics, see, for instance, [24].

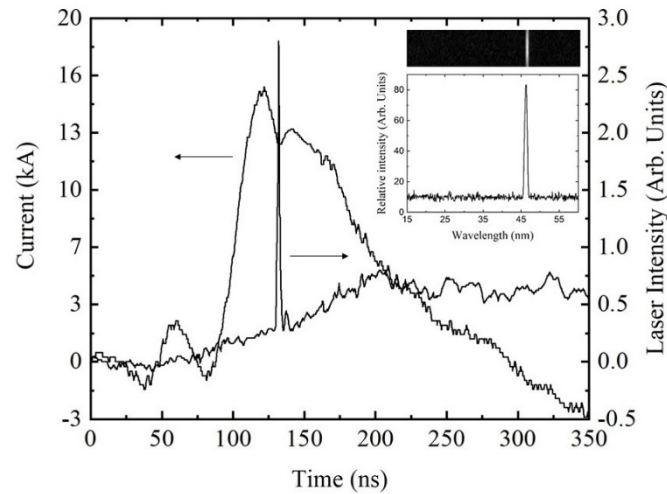
### 3. Experiments and discussions

Figure 3 demonstrates a typical 46.9-nm laser output pulse, excitation current pulse and laser spectra. The de-convoluted duration of the laser pulse recorded by the 100 MHz oscilloscope is 1.6 ns at FWHM. The de-convoluted laser pulse width was estimated using the usual algorithm given by  $\Delta t = [(\Delta t_m)^2 - (\Delta t_{osc})^2]^{1/2}$ , yielding the value  $\Delta t \sim 1.6$  ns. Here,  $\Delta t_m$  is the laser pulse width as measured by the 100 MHz oscilloscope, and  $\Delta t_{osc} = 3.5$  ns is the oscilloscope bandwidth. The laser pulse shown in Fig. 3 has a big pedestal. Because the same pedestal was detected when the laser beam was stopped by a nontransparent obstacle, the pedestal is attributed to electrical background noise. As a result, the background had no effect on the value of laser energy. The sharp kink in the current trace (see Figs. 2 and 3) is induced by an abrupt increase in the inductive resistance of the plasma column during plasma radial compression, as was highlighted in [16]. In the current waveforms (Figs. 2 and 3), there is a small peak between 0 and 50 ns. Although we have not yet examined the physical and technical origins of this peak, it could be attributed to the electrical peculiarities of the charging circuit based on the L-C inversion and magnetic switch compressor (MSC) with voltage inversion on capacitor  $C_1$ . If the peak is eliminated, our future experiments will probably result in a more intense laser.

The peaking capacitor  $C_3$  was charged at a voltage of 35–45 kV. Using our excitation scheme at such a low voltage, the lasing at 46.9 nm (see inset in Fig. 3) was achieved at relatively low (0.18–0.24 mbar) Ar pressures (Fig. 4). These pressures compare well to those published previously for the 46.9-nm lasing at the pressures 0.10–0.37 mbar [23], 0.14–0.22 mbar [32], and 0.12–0.24 mbar [33] which were observed at the use of various excitation techniques with different parameters. It is worth noting that the lasing was also detected previously in the B (69.8 nm) and C (72.6 nm) lines, depending on experimental parameters such as Ar pressure, pre-ionization and excitation pulses, capillary length and diameter, and so on [33–36]. Figure 4 shows the dependence of measured laser energy on argon pressure for three charging voltages, 40, 43 and 45 kV at a pulse repetition rate of 0.1 Hz. The amplitudes of pumping currents corresponding to the charging voltage are 12.3, 14.8, and 17.1 kA, respectively. The laser energy increases with the increase in charging voltage. At the optimal parameters, the charging voltage of 45 kV and argon pressure of 0.21 mbar, the laser energy reaches 4  $\mu$ J. That shows that the twofold decrease of the charging voltage compared to [16] was possible at the expense of an about a factor of three losses in laser output energy.

The computer study of physical reasons why the laser can operate with a lower voltage will be presented in forthcoming works using our (MHD + atomic-kinetic-code) model, for example [24]. Nonetheless, without employing computer models, a simple analysis of the creation of population





**Fig. 3.** Laser output pulse and first half period of excitation current pulse. The sharp kink in the current trace is caused by a rapid increase in the inductive resistance of the plasma during the Z pinch. The laser spectrum is shown in the inset of the figure.

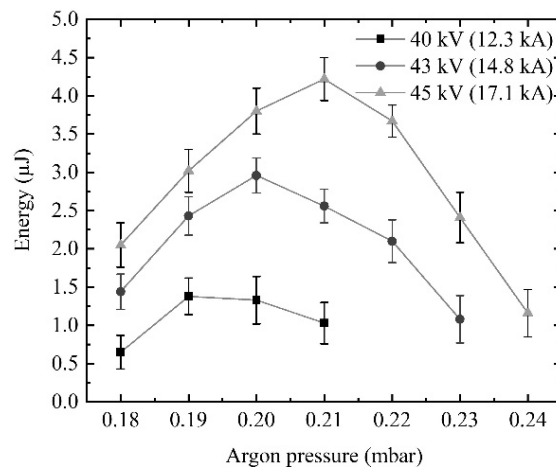


**Fig. 4.** Measured laser energy versus Ar pressure for three charging voltages, 40, 43, and 45 kV, corresponding to pumping currents of 12.3 kA, 14.8 kA, and 17.1 kA, respectively.

inversion on the laser transitions provides a meaningful explanation of low-voltage lasing. Indeed, using our low-voltage excitation approach reduced the rise time of pumping current to a very modest value of  $\sim 15$  ns. At a current peak value of 17 kA, the slope of the excitation current is  $>10^{12}$  A/s, which is remarkably large in contrast to comparable excitation systems. This results in faster plasma detachment from the capillary and more effective formation of Z-pinch with high density and temperature of electrons near the axis of the plasma column at the final stage of plasma compression, which is optimal for 46.9-nm lasing with Gauss intensity distribution. Excitation schemes that generate pumping currents with longer rise times, or the use of longer capillaries and various pre-pulse (pre-ionization) currents, provide lasing in the 46.9-nm line as well as the B (69.8 nm) and C (72.6 nm) lines at lower electron densities and temperatures. The intensive discharge ablation of the capillary walls over a large number of pulses increases their

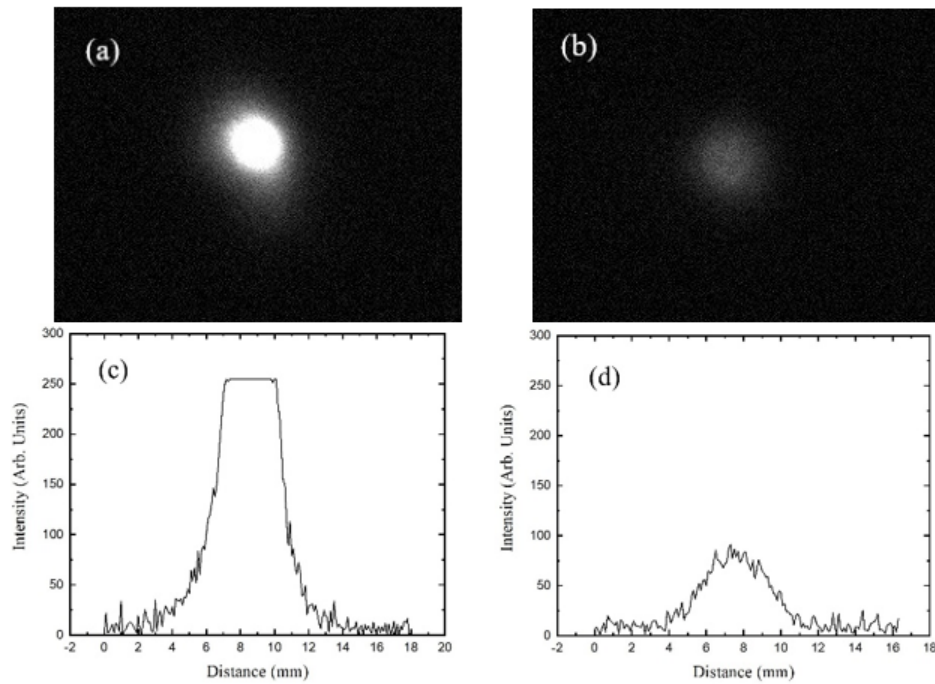


**Fig. 5.** Far-field time-integrated images of the laser beam measured at 180 cm from the capillary exit without (a) and with (b) Al-foil intensity attenuator. Intensity profiles (c) and (d), respectively.

surface roughness, reducing plasma column homogeneity. As mentioned in [37], decreasing the rise time minimizes capillary wall ablation and hence decreases capillary wall ablation and increases capillary life time. In this regard, it is worth noting that the role of wall ablation in plastic and ceramic capillaries on  $\text{Ar}^{+8}$ -laser operation has been studied, for example, in [38]. The fast detachment of plasma from the capillary wall could also be related to the relatively high stability of the discharge (Fig. 2) and laser (Fig. 3) pulses, which decreases slightly with the number of applied pumping pulses. The vertical bars at the measurement positions in Fig. 3 show the shot-to-shot stability of laser pulse energy obtained for five excitation pulses. We note that when the laser pulse energy decreases, so does the shot-to-shot stability. Although plasma relaxation processes in the  $\mu\text{s}$  range allow for kHz pulse-repetition rates, the laser's maximum pulse-repetition rate and life-time are limited mainly by spark-gap electrode erosion. In principle, switching to semiconductor technology could help solve this problem.

Figure 5 shows the time integrated far-field images of laser beams recorded in a single shot at a distance of 1.8 m from the laser exit for the charging voltage of 45 kV and current of 17.1 kA without and with an Al-foil intensity attenuator of thickness  $0.4 \mu\text{m}$ . The laser beam did pass through the grounded cathode electrode, which has a hole on the axis. Argon was continuously flown at the cathode end of the plasma channel. To avoid considerable attenuation of the laser pulse due to photoionization of Ar atoms, argon was differentially pumped using a standard combination of a scroll pump and a turbo-molecular pump. In Figs. 3 and 5, we note that the spontaneous light emitted by the plasma in hundreds of extreme ultraviolet transitions produces an insignificant background in comparison to the laser beam. The laser generates beams with a Gaussian intensity distribution and an FWHM divergence of approximately 1.9 mrad. Although the 1.9 mrad divergence is comparable to the 5.2 mrad reported in [16] for a 13- $\mu\text{J}$  annular beam, the 4- $\mu\text{J}$  beam with a Gaussian intensity distribution is expected to have better focusing

characteristics and a higher intensity. The maximum laser energy of 4  $\mu\text{J}$  was obtained with the relatively high amplitude (17 kA) of the main discharge current. Further optimization of the discharge parameters may result in a reduction in amplitude to around 9 kA, as demonstrated in the studies [18,23].

It is worth noting that the laser energy increases with increasing voltage up to a maximum of 4  $\mu\text{J}$  (Fig. 4). Further improvements to our low-voltage setup could result in an increase in laser energy of up to  $\sim 10 \mu\text{J}$ . Thus, in applications requiring more than 10  $\mu\text{J}$ , the existing low-voltage laser system cannot replace high-voltage  $\text{Ar}^{+8}$ -laser systems that generate laser pulses with energies up to the mJ level [15,27]. In our case, however, the Gaussian beam with 1.9 mrad divergence and 4  $\mu\text{J}$  energy can be effective in applications that require high-quality beams with relatively high laser intensity rather than energy.

#### 4. Summary and conclusions

We demonstrated the operation of a 46.9-nm capillary discharge  $\text{Ar}^{+8}$ -laser pumped by electrical pulses at a very low voltage (35 – 45 kV), which is about twice as low as previously reported in [16]. The reduction of the charging voltage was possible at the expense of about a factor of three losses in laser output energy. In an Ar-filled alumina capillary with an inner diameter of 3.1 mm and a length of 22 cm, laser pulses with an energy of 4  $\mu\text{J}$  and a duration of 1.6 ns were generated at a pulse repetition rate of  $\sim 0.1$  Hz. The laser beams have a Gaussian intensity distribution with a  $\sim 1.9$  mrad FWHM divergence. While the 1.9 mrad divergence is comparable to the 5.2 mrad reported in [16] for a 13- $\mu\text{J}$  annular beam, the 4- $\mu\text{J}$  beam with a Gaussian intensity distribution should have better focusing capabilities and a higher intensity. The beam focusing properties will be investigated in our future experiments. Although we have not yet modeled the novel (35 – 45 kV) regime of operation of a capillary discharge  $\text{Ar}^{+8}$  laser, future investigations will characterize the laser behavior using our MHD model [24]. The two-fold reduction in pulse voltage not only enables further reduction in the size of the laser's excitation unit, particularly through the use of semiconductor technologies and gliding-discharge pre-ionization, but also a principal shift to the experimental methods, techniques, and technologies that are used in ordinary, very compact TEA gas lasers. The results presented in the current paper could be particularly valuable in the study and development of practical soft x-ray capillary lasers for use in small laboratories at educational and research institutes. By using a simple 35 – 45 kV pumping system, more laboratories will be able to conduct further research on soft x-ray capillary lasers, particularly those that would operate at wavelengths less than 46.9 nm. Although, in applications requiring more than 10  $\mu\text{J}$ , the existing low-voltage laser system cannot replace high-voltage  $\text{Ar}^{+8}$ -laser systems that generate laser pulses with energies up to the mJ level, the Gaussian beam with 1.9 mrad divergence and 4  $\mu\text{J}$  energy can be effective in applications that require high-quality beams with relatively high laser intensity rather than energy.

**Funding.** National Research, Development and Innovation Office (OTKA K138339); Pécsi Tudományegyetem (PTE KAP 014\_2023\_PTE\_RK/9); The Development and Innovation Fund of Hungary (TKP2021-EGA-17) (TKP2021-EGA-17).

**Acknowledgments.** The project has been supported by the Development and Innovation Fund of Hungary, financed under the TKP2021-EGA-17 funding scheme, the Research Fund of the University of Pecs (PTE KAP, contract 014\_2023\_PTE\_RK/9), and the National Research, Development, and Innovation Office of Hungary (OTKA K138339).

**Disclosures.** The authors declare no conflicts of interest.

**Data availability.** Data underlying the results presented in this paper are not publicly available at this time but may be obtained from the authors upon reasonable request.

#### References

1. R. C. Elton, *X-Ray Lasers* (Academic Press, London, 1990).
2. S. Suckewer and P. Jaegle, "X-Ray laser: past, present, and future," *Laser Phys. Lett.* **6**(6), 411–436 (2009).
3. J. Nielson, "X-ray lasers: the evolution from Star Wars to the table-top," *Proc. SPIE* **11886**, 1188604 (2021).



4. B. R. Benware, A. Ozols, J. J. Rocca, I. A. Artioukov, V. V. Kondratenko, and A. V. Vinogradov, "Focusing of a tabletop soft x-ray laser beam and laser ablation," *Opt. Lett.* **24**(23), 1714–1716 (1999).
5. A. Artioukov, B. R. Benware, J. J. Rocca, M. Forsythe, Y. A. Uspenskii, and A. V. Vinogradov, "Determination of XUV optical constants by reflectometry using a high-repetition rate 46.9-nm laser," *IEEE J. Select. Topics Quantum Electron.* **5**(6), 1495–1501 (1999).
6. J. Filevich, K. Kanizay, M. C. Marconi, J. L. A. Chilla, and J. J. Rocca, "Dense plasma diagnostics with an amplitude-division soft-x-ray laser interferometer based on diffraction gratings," *Opt. Lett.* **25**(5), 356–358 (2000).
7. M. Seminario, J. J. Rocca, R. Depine, B. Bach, and B. Bach, "Characterization of Diffraction Gratings by use of a Tabletop Soft-X-Ray Laser," *Appl. Opt.* **40**(30), 5539–5544 (2001).
8. G. Tomassetti, A. Ritucci, A. Reale, L. Palladino, L. Reale, L. Arriza, G. Baldacchini, F. Bonfigli, F. Flora, L. Mezi, R. M. Montereali, S. V. Kukhlevsky, A. Faenov, T. Pikuz, and J. Kaiser, "High-resolution imaging of a soft-X-ray laser beam by color centers excitation in lithium fluoride crystals," *Europhys. Lett.* **63**(5), 681–686 (2003).
9. M. G. Capeluto, P. Wachulak, M. C. Marconi, D. Patel, C. S. Menoni, J. J. Rocca, C. Lemmi, E. H. Anderson, W. Chao, and D. T. Attwood, "Table top nanopatterning with extreme ultraviolet laser illumination," *Microelectron. Eng.* **84**(5-8), 721–724 (2007).
10. Y. Zhao, H. Cui, W. Zhang, W. Li, S. Jiang, and L. Li, "Si and Cu ablation with a 46.9-nm laser focused by a toroidal mirror," *Opt. Express* **23**(11), 14126–14134 (2015).
11. S. Suckewer, A. V. Sokolov, and M. O. Scully, "Compact X-ray laser amplifier in the "Water Window"," *Spectrochim. Acta, Part A* **255**(5), 119675 (2021).
12. J. J. Rocca, V. Shlyaptsev, F. G. Tomasel, O. D. Cortázar, D. Hartshorn, and J. L. A. Chilla, "Demonstration of a Discharge Pumped Table-Top Soft-X-Ray Laser," *Phys. Rev. Lett.* **73**(16), 2192–2195 (1994).
13. J. J. Rocca, D. P. Clark, J. L. A. Chilla, and V. N. Shlyaptsev, "Energy Extraction and Achievement of the Saturation Limit in a Discharge-Pumped Table-Top Soft X-Ray Amplifier," *Phys. Rev. Lett.* **77**(8), 1476–1479 (1996).
14. B. R. Benware, C. D. Macchietto, C. H. Moreno, and J. J. Rocca, "Demonstration of a High Average Power Tabletop Soft X-Ray Laser," *Phys. Rev. Lett.* **81**(26), 5804–5807 (1998).
15. C. D. Macchietto, B. R. Benware, and J. J. Rocca, "Generation of millijoule-level soft-x-ray laser pulses at a 4-Hz repetition rate in a highly saturated tabletop capillary discharge amplifier," *Opt. Lett.* **24**(16), 1115–1117 (1999).
16. S. Heinbuch, M. Grisham, D. Martz, and J. J. Rocca, "Demonstration of a desk-top size high repetition rate soft x-ray laser," *Opt. Express* **13**(11), 4050–4055 (2005).
17. A. Ben-Kish, M. Shuker, R. A. Nemirovsky, A. Fisher, A. Ron, and J. L. Schwob, "Plasma Dynamics in Capillary Discharge Soft X-Ray Lasers," *Phys. Rev. Lett.* **87**(1), 015002 (2001).
18. G. Niimi, Y. Hayashi, N. Sakamoto, M. Nakajima, A. Okino, M. Watanabe, K. Horioka, and E. Hotta, "Development and Characterization of a Low Current Capillary Discharge for X-ray Laser Studies," *IEEE Trans. Plasma Sci.* **30**(2), 616–621 (2002).
19. A. Ritucci, G. Tomassetti, A. Reale, L. Palladino, L. Reale, F. Flora, L. Mezi, S. V. Kukhlevsky, A. Faenov, and T. Pikuz, "Investigation of a highly saturated soft x-ray amplification in a capillary discharge plasma waveguide," *Appl. Phys. B: Lasers Opt.* **78**(7-8), 965–969 (2004).
20. K. Kolacek, J. Schmidt, V. Prukner, J. Straus, O. Frolov, and M. Martinkova, "Research on high current pulse discharges at IPP ASci CR," *Czech. J. Phys.* **56**(S2), B259–B266 (2006).
21. V. I. Ostashev, A. M. Gafarov, V. Y. Politov, A. N. Shushlebin, and L. V. Antonova, "Evidence of Soft X-Ray Lasing in SIGNAL Pulsed-Power Facility Experiments with Argon Capillary Plasma," *IEEE Trans. Plasma Sci.* **34**(5), 2368–2376 (2006).
22. Y. Zhao, Y. Cheng, B. Luan, Y. Wu, and Q. Wang, "Effects of capillary discharge current on the time of lasing onset of soft x-ray laser at low pressure," *J. Phys. D: Appl. Phys.* **39**(2), 342–346 (2006).
23. C. A. Tan and K. H. Kwek, "Development of a low current discharge-driven soft x-ray laser," *J. Phys. D: Appl. Phys.* **40**(16), 4787–4792 (2007).
24. J. Szasz, M. Kiss, I. Santa, S. Szatmari, and S. V. Kukhlevsky, "Magnetoelectric Confinement and Stabilization of Z Pinch in a Soft-X-Ray Ar<sup>+8</sup> Laser," *Phys. Rev. Lett.* **110**(18), 183902 (2013).
25. Y. Zhao, S. Jiang, H. Cui, L. Li, W. Zhang, and W. Li, "Influence of the gain-length product on the pulse duration of highly saturated capillary discharge soft X-ray laser," *Appl. Phys. B* **121**(1), 87–93 (2015).
26. S. Barnwal, S. Nigam, K. Aneesh, Y. B. S. R. Prasad, A. S. Joshi, and P. A. Naik, "Impact of discharge current profile on the lasing efficiency of 46.9 nm capillary discharge soft x-ray laser," *Laser Phys.* **27**(5), 055003 (2017).
27. M. U. Khan, Y. Zhao, T. Hui, M. K. Shahzad, H. Cui, and D. Zhao, "Impact of discharge currents on the intensity of 46.9 nm capillary discharge soft X-ray laser," *Opt. Express* **27**(12), 16738–16750 (2019).
28. Y. Zhao, D. Zhao, Q. Yu, M. U. Khan, H. Lu, J. Li, and H. Cui, "Influence of He mixture on the pulse amplitude and spatial distribution of an Ne-like Ar 46.9 nm laser under gain saturation," *J. Opt. Soc. Am. B* **37**(8), 2271–2277 (2020).
29. M. U. Khan, Y. Zhao, H. Cui, F. Zhang, Z. Cao, and B. An, "Operation and output pulse characteristics of a discharge-pumped 46.9 nm soft X-ray laser with larger inner diameter capillary and higher discharge currents," *Eur. Phys. J. Plus* **136**(6), 628–643 (2021).
30. S. Szatmari, J. Bohus, Z. Gao, X. Tang, and N. Wang, "Three-channel KrF laser with distributed magnetic switch-based charging circuit," *Rev. Sci. Instrum.* **77**(11), 115106 (2006).

31. S. Szatmari, "Short-pulse KrF amplifier using spatially tunable x-ray preionization," *Rev. Sci. Instrum.* **91**(4), 043001 (2020).
32. S. Jiang, Y. Zhao, Y. Xie, M. Xu, H. Cui, H. Wu, Y. Liu, Q. Xu, and Q. Wang, "Observation of capillary discharge Ne-like Ar 46.9 nm laser with pre-pulse and main-pulse delay time in the domain of 2–130  $\mu$ s," *Appl. Phys. B* **109**(1), 1–7 (2012).
33. Y. Zhao, T. Liu, S. Jiang, H. Cui, Y. Ding, and L. Li, "Characteristics of a multi-wavelength Ne-like Ar laser excited by capillary discharge," *Appl. Phys. B* **122**(5), 107 (2016).
34. Y. Zhao, T. Liu, W. Zhang, W. Li, and H. Cui, "Demonstration of gain saturation and double-pass amplification of a 69.8 nm laser pumped by capillary discharge," *Opt. Lett.* **41**(16), 3779–3782 (2016).
35. T. Liu, Y. Zhao, H. Cui, and X. Liu, "Characteristics of gain in Ne-like Ar 69.8 nm laser pumped by capillary discharge based on double-pass amplification," *Acta Phys. Sin.* **68**(2), 025201 (2019).
36. Y. Bai, Y. Zhao, B. An, D. Zhao, H. Cui, L. Li, and J. Li, "Effects of pre-pulse current on Ne-like Ar laser at 72.6 nm excited by capillary discharge," *Appl. Phys. B* **128**(9), 163 (2022).
37. J. J. Rocca and A. V. Vinogradov, "Repetitively pulsed X-ray laser operating on the 3p-3s transition of the Ne-like argon in a capillary discharge," *Quantum Electron.* **33**(1), 7–17 (2003).
38. A. Ritucci, G. Tomassetti, A. Reale, L. Palladino, L. Reale, T. Limongi, F. Flora, L. Mezi, S. V. Khuklevsky, A. Faenov, T. Pikuz, and J. Kaiser, "Role of the wall ablation in the operation of a 46.9 nm Ar capillary discharge soft x-ray laser," *Contrib. Plasma Phys.* **43**(2), 88–93 (2003).